

FINAL
03-1939

An Overview of the Nuclear Electric Xenon Ion System (NEXIS) Program *

J. E. Polk, D. Goebel, J. R. Brophy, J. Beatty
Jet Propulsion Laboratory, M/S 125-109, 4800 Oak Grove Drive, Pasadena, CA 91109
(818) 354-9275, james.e.polk@jpl.nasa.gov

J. Monheiser, D. Giles, D. Hobson, F. Wilson
Aerojet-Redmond Operations, Redmond, Washington

J. Christensen, M. De Pano, S. Hart
Boeing Electron Dynamic Devices, Inc., Torrance, California

W. Ohlinger
Consultant, Pittsburgh, Pennsylvania

D.N. Hill
Georgia Institute of Technology, Atlanta, Georgia

J. Williams, P. Wilbur, D.M. Laufer and C. Farnell
Colorado State University, Fort Collins, Colorado

AIAA-2003-4713[†]

NASA is investigating high power, high specific impulse propulsion technologies that could enable ambitious flights such as multi-body rendezvous missions, outer planet orbiters and interstellar precursor missions. The requirements for these missions are much more demanding than those for state-of-the-art solar-powered ion propulsion applications. The purpose of the NEXIS program is to develop advanced ion thruster technologies that satisfy the requirements for high power, high specific impulse operation, high efficiency and long thruster life. The nominal design point for the NEXIS thruster is 20 kWe at a specific impulse of 7500 s with an efficiency over 78% and a xenon throughput capability of greater than 2000 kg. These performance and throughput goals will be achieved by applying a combination of advanced technologies including a large discharge chamber, erosion resistant carbon-carbon grids, an advanced reservoir hollow cathode and techniques for increasing propellant efficiency such as grid masking and accelerator grid aperture diameter tailoring. This paper provides an overview of the challenges associated with these requirements and how they are being addressed in the NEXIS program.

* Copyright ©2003 by the American Institute of Aeronautics and Astronautics, Inc. The U.S. Government has a royalty-free license to exercise all rights under the copyright claimed herein for Governmental purposes. All other rights are reserved by the copyright owner.

[†] Presented at the 2003 Joint Propulsion Conference, Huntsville, AL, July 20-23, 2003.

Introduction

The demonstration of ion propulsion on the Deep Space 1 mission has paved the way for applications of advanced electric propulsion on more demanding future missions such as outer planet orbiters, multiple body rendezvous missions, sample return

missions and interstellar precursor flights. However, these exciting missions place much greater demands on the propulsion system, as shown in Fig. (1) [1]. The chemical propulsion systems that have been used on most planetary missions to date have delivered ΔV s of a few km/s. Near-term missions demanding ΔV s of 10-40 km/s can be accomplished using Solar Electric Propulsion (SEP) systems processing between 10 and 25 kWe with specific impulses of 3000-5000 s. More ambitious missions require ΔV s ranging from 40 to over 100 km/s. To accomplish these missions with reasonable initial masses and tolerable trip times requires advanced Nuclear Electric Propulsion (NEP) systems capable of processing from 100 to 500 kWe of power at I_{sp} 's ranging from 5000 s to over 14000 s [1, 2]. The burn times for these missions range from five to ten years. Future ion propulsion systems must therefore operate at higher power levels, higher I_{sp} 's and with longer lifetimes than state-of-the-art SEP systems.

The Nuclear Electric Xenon Ion System (NEXIS) technology program was proposed in response to a NASA Research Announcement (NRA) soliciting proposals to identify and develop high power thruster technologies that enable NEP missions to the outer planets. The NEXIS team is led by the Jet Propulsion Laboratory (JPL) with partners Aerojet, the Aerospace Corporation, Boeing, Colorado State University, Georgia Tech, the Marshall Spaceflight Center, the University of Michigan, MIT and Virginia Polytechnic Institute. A conceptual design study was recently completed during a six month Phase 1 effort, and a 2 year second phase focused on developing and demonstrating the NEXIS technologies is just beginning.

The goal of the NRA is to demonstrate a thruster that meets the following performance objectives:

1. Power per thruster of 20-50 kWe for use in vehicles with total system power up to 100 kWe
 2. Specific impulse of 6000 s to 9000 s.
 3. Total efficiency exceeding 65%.
 4. Thruster specific mass consistent with a total power and propulsion system specific mass of 35 kg/kWe.
 5. Propellant throughput capability of 50 kg/kWe.
- These technologies are also of interest for the Jupiter

Icy Moons Orbiter (JIMO) mission under consideration by NASA for a launch as early as 2011. The NEXIS program is therefore also focused on addressing the specific needs of this potential near-term application of NEP.

The purpose of this paper is provide an overview of the NEXIS program, including the technical challenges associated with satisfying the requirements and the types of technologies to be applied in meeting those challenges.

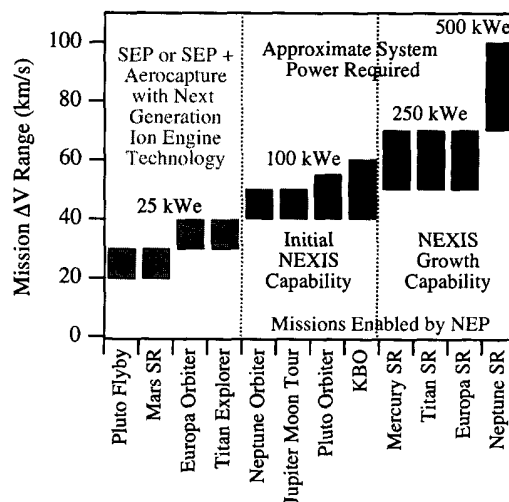


Figure 1: NEP enables missions with $\Delta V \geq 40$ km/s (SR refers to Sample Return missions).

Overview of the NEXIS Technology Development Approach

The purpose of the NEXIS program is to develop the ion thruster technology base required for an NEP vehicle and to prepare industry to bid competitively on a subsequent advanced development effort.

Technology Trade Studies

A number of approaches to meeting these requirements were considered as shown in the trade tree in Fig. (2). A DC discharge chamber with carbon grids, xenon propellant and advanced

reservoir hollow cathodes was chosen as the best balance between performance, life and development risk. Although many different ion source types

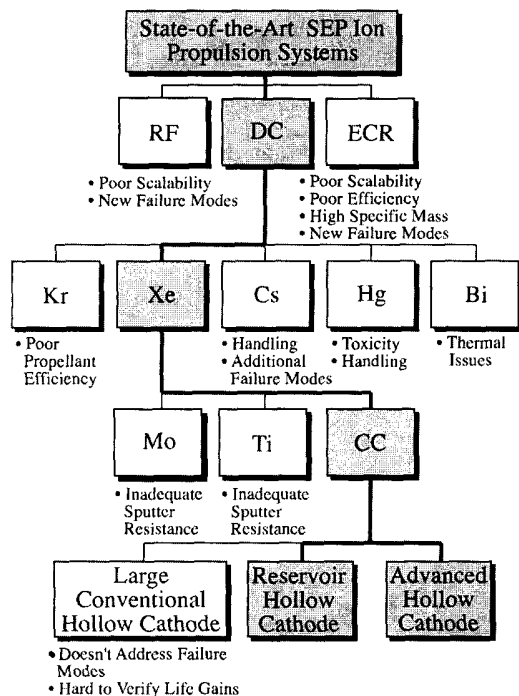


Figure 2: High power ion thruster trade space. Shaded boxes represent the NEXIS approach.

are in development, only three are sufficiently mature to be considered. Radio frequency (RF) and microwave electron cyclotron resonance (ECR) thrusters are potentially attractive because they do not use thermionic cathodes, which in principle can limit the life of thrusters with DC discharges. However, these approaches were rejected because of poor scalability to large chambers, poor SOA efficiency, high specific mass and low efficiency of the power supplies and the potential for new failure modes [3, 4, 5].

Xenon was chosen because it yields the best combination of performance potential and ease of handling. For cesium, a highly reactive alkali metal, the potential performance gain does not justify the handling difficulty. Bismuth is not particularly reac-

tive, but condenses on the thruster if it is not maintained at about 1000 degrees C. This is an unacceptable thermal issue for large area ion thrusters, but Bi looks very attractive for high power anode layer thrusters [6]. Mercury was rejected because of its toxicity and difficulty in controlling low flow rates. Condensable propellants may yield higher performance and have much lower facility pumping speed requirements. However, the modest flow rates required for the NEXIS thruster can be accommodated with existing test facilities.

Extraordinarily long burn times drove the grid material selection to carbon, which has the lowest sputter yield of any candidate material. Given advances in carbon-carbon composite grid technology [7, 8] there is no compelling reason not to use the material with the greatest life capability.

Simply scaling hollow cathodes to larger dimensions was rejected because this approach is not expected to yield the necessary gain in lifetime. Dimensional scaling does not address the fundamental insert chemistry, which is the key determinant of lifetime. Finally, the lifetime of conventional impregnated insert cathodes can only be demonstrated in full-duration life tests. In contrast, the NEXIS reservoir cathode addresses all critical insert failure modes and allows accelerated testing to establish life capability. Advanced hollow cathodes incorporating new materials but using established insert fabrication methods do not offer all of the advantages of the reservoir cathode, but will be pursued in parallel as a lower risk, lower payoff option.

Overview of the NEXIS Design

Table 1 shows the nominal NEXIS thruster design operating point, which is a significant step beyond the state-of-the-art NASA Solar Electric Propulsion (SEP) Technology Applications Readiness (NSTAR) ion thruster, which was demonstrated on the Deep Space 1 (DS1) mission [9]. The power processing capability, specific impulse and efficiency are all increased dramatically. Perhaps more importantly, all known wear out failure modes are eliminated by exploiting advanced grids constructed from erosion-resistant carbon-carbon, a new

reservoir hollow cathode, and a new large-diameter discharge chamber. These performance and life objectives meet or exceed the requirements of the NASA Research Announcement. A further goal of the NEXIS program is to demonstrate the flexibility of the technologies to operate over a wide range of operating conditions of interest to future missions.

The NEXIS thruster shown in Fig. (3) has a 65-cm diameter discharge chamber with six rings of magnets in a ring-cusp configuration. Improved plasma uniformity relative to the state-of-the-art (SOA) is used to enhance grid life. In the NEXIS thruster this is achieved by controlling the fringing of the magnetic field at the downstream magnet ring and masking the chamber to produce a 57-cm diameter ion beam. Efficiency $\geq 78\%$ is achieved by signif-

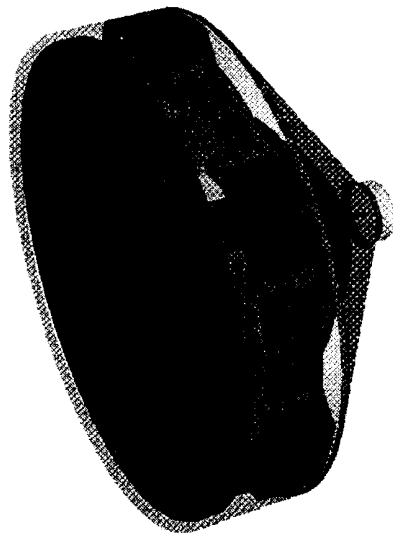


Figure 3: Overview of the NEXIS thruster design.

icantly improving propellant utilization through the use of a deep discharge chamber, tailoring the accelerator grid apertures to the radial variation in beamlet size, and sharing the neutralizer function between multiple thrusters. A key feature is that this approach increases the propellant efficiency without increasing double ion content or discharge voltage.

Exceptionally long grid life is achieved by using

carbon grids, derating the peak beam current density to less than half the NSTAR/DS1 value, and designing the grids to operate with a very high perveance margin. Operation with a large perveance margin focuses more of the charge-exchange ions produced between the grids out through the accelerator grid, minimizing the sputter-erosion of the accelerator grid hole walls. Exceptionally long cathode life is achieved by lowering the temperature of the emitter and increasing the amount of low work function material contained in the cathode. The NEXIS thruster uses a reservoir cathode with a W-Ir emitter that will lower the emitter temperature, significantly increasing life. In addition, the reservoir cathode includes 10 times the quantity of low work function material than SOA cathodes, further improving the cathode life.

These design choices were driven by the requirements for high power, high specific impulse operation, long grid and cathode life, and high efficiency. The particular technical challenges and the strategies for addressing them are outlined in the following three sections.

High Power, High Specific Impulse Operation

For a given propellant, higher Isp is achieved with higher beam voltage, V_b . The thruster size was chosen to allow operation at a range of Isp and power levels while still meeting the throughput requirements.

Technical Challenges

The key to high power, high Isp thrusters is the grid design. Challenges include developing a geometry that extracts the required current density with proper beamlet focusing over the range of plasma densities produced upstream of the grids with a realistic electric field. Underfocusing in the high density regions in the center of the grid and overfocusing at the periphery can cause direct ion impingement on the hole walls in the downstream grid. In addition, the voltage on the downstream grid must be chosen to prevent electron backstreaming. Finally, the grids must be designed to minimize the dynamic loads encountered during launch. Higher voltages

Performance Metric	State-of-the-Art SEP Thrusters (NSTAR)	NEXIS Thruster	
		Nominal Design	Gain Over SOA
Power (kWe)	2.3	20	9X
Isp (s)	3170	7500	2.4X
Thruster Efficiency	0.63	0.78	1.25X
Specific Mass (kg/kWe)	3.6	1.5	2.4X less
Throughput (kg)	230	2000	8.7X
Service Life (khrs)	30	93	3X

Table 1: The NEXIS thruster technology is a significant advance to the state of the art.

necessitate improved isolation in the thruster and create lifetime challenges that are discussed in the next section. The magnets are not considered a development risk. High power is processed in a large discharge chamber with low beam current density, and preliminary thermal analysis indicates that the heat flux to the magnets is less than in SOA thrusters.

Solutions

A number of innovations allow these challenges to be met. New ion optics simulation tools and detailed structural modeling of grids fabricated from carbon-carbon composites have provided the insight to design long-life, high performance grids. These challenges will be addressed by three major approaches.

1. *Sophisticated ion optics design tools.* Grid designs can now be more affordably developed using state-of-the-art 2D and 3D plasma simulation tools that have been validated with data [10]. These codes accurately calculate the upstream grid transparency to ions, the ion beamlet current density, the ion trajectories and the electrostatic potentials required to prevent electron backstreaming. They also model the generation, flow and resulting grid erosion of ions created by charge exchange reactions between beam ions and neutral xenon. Candidate designs were developed by evaluating simulation results for dozens of potential geometries and voltages. The NEXIS team has identified viable grid designs for a range of Isp's for both near-term and mid-term NEP missions. The codes were used to identify

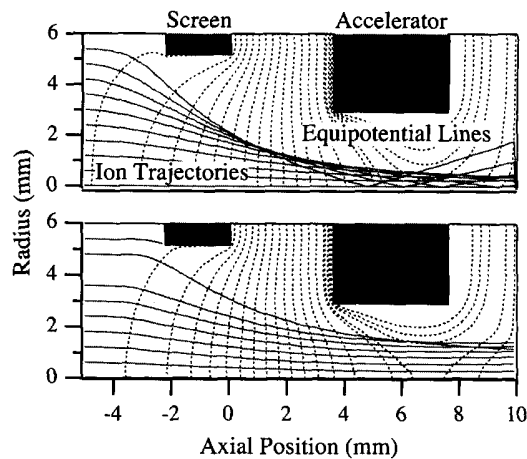


Figure 4: The NEXIS grid design provides proper beamlet focusing at low densities (top) and high densities (bottom).

candidate designs that yield the required range of current densities without direct impingement. For example, Fig. (4) shows proper focusing of a beamlet through a single aperture for the two bounding cases most susceptible to direct ion impingement. The simulation results were subsequently verified for several different grid designs in subscale grid tests, as shown in Fig. (5). These plots show the ratio of accelerator grid impingement current to beam current as a function of beamlet current measured for the NEXIS designs in subscale tests of optics designs optimized for Isp's of 7500 and 9000 s. These data were obtained by operating subscale

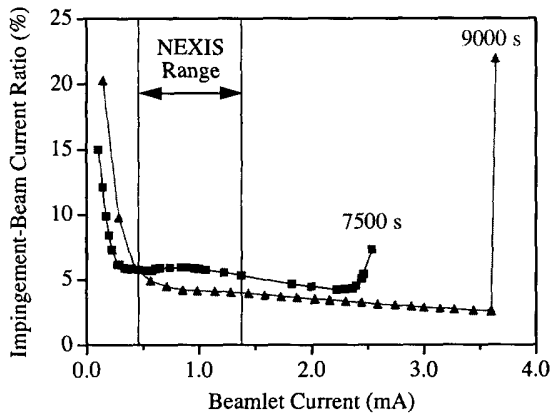


Figure 5: Beam extraction tests with subscale NEXIS grids validate geometries designed using the computer simulation tools.

carbon-carbon gridlets on a small ion source at Colorado State University [11]. The ratio of accelerator grid current to beam current rises at low beamlet currents (which corresponds to low upstream plasma densities) because of direct impingement due to overfocusing and at high beamlet currents (high densities) because of underfocusing. The peak beamlet currents required by the candidate designs are about 4–5 times higher than the crossover limits. These dynamic ranges can be accommodated by carefully designing the discharge chamber to achieve a relatively uniform plasma density profile.

Subscale tests over a range of specific impulses were also performed with the grids designed for a nominal Isp of 7500 s. As Fig. (6) shows, Isp's between at least 6000 and 9000 s can be accommodated with this single grid design simply by changing the grid gap. Comparison of the operating limits for the 9000 s cases in Fig. (5) and Fig. (6) shows that the optimized grid design offers a higher perveance limit, but the perveance limits of both designs are above the peak beamlet current required by NEXIS. This demonstrates that the NEXIS grid designs offer great flexibility in meeting evolving requirements for NEP missions. Full-scale tests will be performed with the nominal 7500 s grid design over a range of Isp's and with designs optimized for other spe-

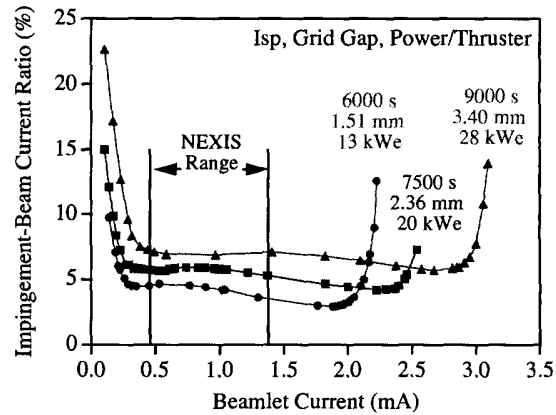


Figure 6: Subscale grid tests show that the NEXIS 7500 s grid design will operate over a broad range of Isp's just by changing the grid gap.

cific impulses. Figure (7) shows a first generation flat carbon-carbon grid machined with the nominal NEXIS screen grid hole pattern which will be used in initial tests of a laboratory model thruster.

2. *Structurally robust grids.* The key to surviving launch loads is the structural design. Fortunately, high Isp operation drives the grid design to be very robust with considerable structural margin. The grids are very thick, spaced far apart, and the minimum webbing width between apertures is large. Three-dimensional finite element models have been used to design 30-cm and 75-cm grids [7] and are now being applied to the NEXIS design. The primary design variables are the dish depth and the screen grid boundary constraint. Conventional molybdenum grids are dished so that both grids buckle in the same direction as they get hot, helping maintain the desired grid gap. Carbon-carbon has a coefficient of thermal expansion near zero, so thermal buckling is not a concern. However, large carbon-carbon grids must be dished to increase their stiffness. The accelerator grid and the screen grid with its mounting system are modeled separately. These models do not include the apertures machined into the grids or the inherently non-isotropic properties of the composite material. Instead, the properties of the laminate are estimated using standard micromechanics methods

and additional detailed finite element models of local regions of the grids including the apertures are used to determine the effect of the holes on the properties of the composite. These results are then used to define effective properties of an equivalent homogeneous material with no apertures. The damping ratio used in the dynamic simulations is based on measurements of 30 cm diameter slotted grids.

In 30 cm diameter optics, contact between the grids due to launch vibrations produces stresses that can cause them to fail [7]. Failure is avoided by designing the grids with sufficient stiffness that they do not contact each other during launch. Simulations of loads representative of a Delta IV Heavy launch on 75-cm diameter optics showed that the grids do not contact each other, but that the screen grid may be damaged by stresses induced by deflections. The screen grid is more susceptible to damage than the accelerator grid because its higher open area fraction results in lower strength. A range of dish depths was studied, and a 76 mm dish depth yielded a margin of safety, defined as $MOS = (\text{allowable stress} - \text{calculated stress}) / \text{calculated stress}$, of 0.79. This MOS should accommodate any uncertainties in loads and variability in manufacturing. The current NEXIS grid design is similar to the 75 cm grid design and incorporates this same dish depth, but this may be adjusted to provide the required MOS on the basis of ongoing structural analyses for this particular design.

The constraints at the periphery of the screen grid were also varied in 30 and 75 cm grid analyses, and the results showed that bonding the screen grid to a very stiff structure can significantly impact the results. The structure currently being used in the grids under development for the NEXIS program is similar to that developed for the 30 cm optics [7].

3. *Innovative isolator designs.* Boeing has over 28 years of high voltage design experience for space systems, which is being exploited in the development of the NEXIS thruster. Two options for high voltage propellant isolators have been studied. Several designs using tortuous passages through a dielectric plug were tested and demonstrated either too low a voltage standoff capability or ≤ 10 kV standoff at the required xenon pressures and flowrates only with very large pressure drops. The isolator design used

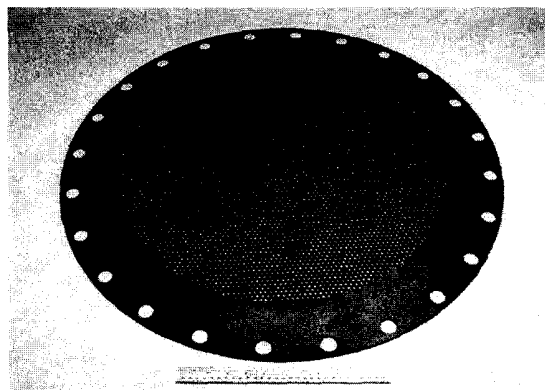


Figure 7: Full scale flat NEXIS grid that will be used in initial laboratory model tests.

in the NSTAR thruster [12] will be scaled to higher voltage capability and used in the NEXIS thrusters.

Long Grid Lifetime

Technical Challenges

NEP applications require a xenon throughput capability as high as 100 kg/kWe, placing great demands on grid lifetime. Most of the relevant grid wear out failure modes are driven by ion-induced sputtering. The NEXIS grids are designed to minimize the flux and energy of ions that strike the grids and to use wear-resistant carbon. SOA modeling tools show that these approaches should eliminate grid wear out as a concern for the NEXIS thruster. The five potential wear out failure modes are [13]:

1. Structural failure of the accelerator grid due to charge exchange (CEX) ion erosion on the downstream surface.
2. Electron backstreaming or structural failure caused by enlargement of the accelerator grid holes from CEX ion erosion.
3. Structural failure of the screen grid due to erosion from discharge ion bombardment.
4. Electrical shorts between the grids by flakes spalled off of thin films of erosion products deposited inside the engine.
5. Continuous arcing due to inadequate voltage standoff capability between the grids.

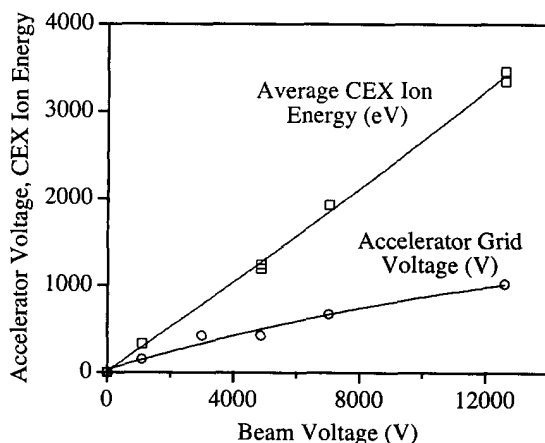


Figure 8: The average energy of the CEX ions hitting the walls of the accelerator grid holes increases linearly with beam voltage.

High voltages required for NEP missions can aggravate some of these processes. Figure (8) shows the accelerator grid voltage and the average energy of ions hitting the accelerator grid hole walls as a function of beam voltage. These values were calculated using ion optics simulation tools that accurately predict the grid erosion rates in the NSTAR thruster. While the grid voltage required to prevent electron backstreaming increases very slowly with beam voltage, the energy of ions hitting the hole walls increases dramatically. Because the majority of these ions are created between the grids, their energy is influenced by both the accelerator grid voltage and the beam voltage. This under-appreciated fact makes it imperative that grids for high Isp applications be as sputter-resistant as possible, and essentially eliminates materials such as molybdenum and titanium as options for long life. Verifying that new designs have sufficient life is also a challenge. In an NEP development program there will not be sufficient time and resources to life test for the full burn time.

Solutions

These challenges will be addressed with strategies that reduce erosion to insignificant levels:

1. *Use of carbon-carbon grids.* Carbon grids have a mass loss rate 4-10 times lower than SOA molybdenum grids [14, 15]. Carbon-carbon (CC) grids were originally developed by JPL [16, 17, 18, 19, 20, 21] and graphite grids are used routinely in ion sources for ground applications. Boeing is currently developing pyrolytic graphite grids for their commercial 13-cm and 25-cm thrusters as well as 30-cm grids for planetary missions [7]. The Japanese Space Agency is currently flying 10-cm CC grids on the Muses-C mission [3] and is developing 20-cm grids [22]. They tested the 10-cm grids for more than 18,000 hours and observed very little erosion [3, 23]. Similar results were achieved in more than 3200 hours of testing with 15-cm grids at JPL [19]. JPL is developing CC grids for 30-cm and 40-cm thrusters under the Carbon-Based Ion Optics (CBIO) program [7] and for NASA GRCs 75-cm interstellar ion thruster [24]. Given the tremendous lifetime benefit, relative maturity and level of complementary development activity it is clear that carbon is the appropriate choice of grid material. The use of carbon is essential to offset the increase in energy of CEX ions striking the grid hole walls noted in Fig. (8).

2. *Derating by use of very low beam current density.* The flux of ions to the grid is minimized by operating at low current densities. The chosen grid area results in an average current density of 1.51 mA/cm² and a peak density of 2.52 mA/cm². This is 46% of the peak density of NSTAR at full power [25] and even less than that of the MUSES-C thruster that completed an 18,000 hour test with very little erosion of the CC grids [3, 23].

3. *Reducing energy of ions striking hole walls by operating with high perveance margin (low plasma density and high voltage, so that ions are strongly focused).* The shaded regions in Fig. (9) are areas where CEX ions which ultimately strike the hole walls are generated for the high and low current density cases shown in Fig. (9). In the upper plot of Fig. (9), higher current density yields less perveance margin, and many of the CEX ions created in the grid gap hit the hole wall. These ions are created at a much higher potential than the grid, and strike the hole wall with energies as high as 6000 eV (for

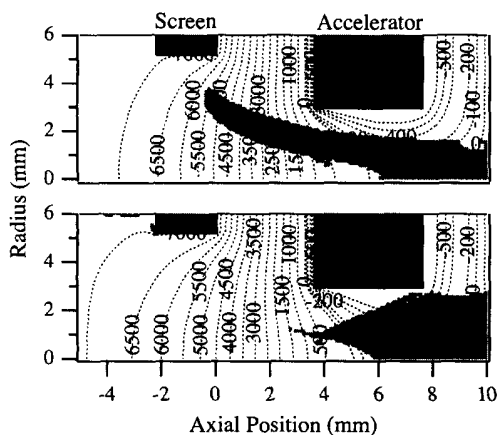


Figure 9: The production location of CEX ions that hit the accelerator grid hole wall is indicated by the green shading. At low perveance margin (top) many CEX ions are produced between the grids at high potential. At high perveance margin (bottom) these ions get focused through the grid aperture.

operation at 9000 s) and an average energy of 2100 eV. In contrast, at lower current density, as shown in the lower plot, high perveance margin results in strong focusing and very few CEX ions from the grid gap strike the hole wall. CEX ions are still formed between the grids, but the strong focusing accelerates them through the downstream grid hole. Consequently, the average energy of the CEX ions hitting the grid hole wall in the lower plot is only 740 eV. Unfortunately, operation with this much perveance margin is not practical because of the very low current density, but the effect is important. Operation with high perveance margin (low plasma density and high voltage, so that ions are strongly focused) minimizes the energy of the CEX ions hitting the hole walls. This effect was exploited in the optics design for NEXIS.

4. *Thick, widely spaced grid design.* High voltage operation enables use of accelerator and screen grids that are eight and five times thicker than the NSTAR grids, respectively, so structural failure due to erosion is not a concern. Low erosion rates of sputter-resistant materials and the large grid gap required by high Isp essentially eliminate the risk of

grid shorts by flakes of sputter-deposited material.

5. *Innovative life assessment tools.* Models of downstream accelerator grid erosion [10] and a new model of hole wall erosion yield excellent agreement with NSTAR data [26]. These models indicate an accelerator grid throughput capability of 4800 - 5000 kg, or 250 kg/kWe, at the nominal operating point. Screen grid erosion models validated with NSTAR data show that with xenon, carbon grids, discharge voltages of 25 V or lower and double ion fractions similar to those in the NSTAR thruster [27, 28], screen grid erosion is not a credible failure. These high fidelity failure models confirm that carbon is so erosion-resistant it will virtually eliminate grid wear-out as a concern, even at high Isp. They will serve as the main basis of life assessment [29, 30, 31, 32] for the NEXIS program.

6. *Use of arc-resistant surface treatments and arc energy limitation to achieve high voltage standoff capability.* Laboratory tests at JPL of the voltage standoff capability of the carbon-carbon composite grid material show that the as-manufactured material can withstand electric fields of well over 10 kV/mm without breakdown. Machining of the apertures in the grid material can degrade this voltage standoff unless care is taken to avoid damage to the webbing between adjacent grid apertures that results in field enhancement at sharp points. Examination of grids with laser machined holes and a proprietary surface treatment indicates that excellent surfaces are maintained and still provide high voltage standoff capabilities of this material. The grid gap spacings in NEXIS are also sufficiently large that normal tolerance of the grid gap dimensions will not result in any significant degradation of voltage hold off. However, during operation the grids are subject to ion bombardment and erosion of the surface. While testing is required to determine the extent of this potential problem, we expect that the voltage hold off capabilities of the surface will be degraded with time. To avoid spurious surface breakdown later in life as the surface evolves, we have designed the grid gap for a relatively low electric field which is below the threshold breakdown fields found for the CC surfaces prior to the surface treatment process. This means that even if the ion bombardment

degrades the treated surface to the unprocessed level, the grids will still have sufficient margin to avoid arcing and breakdown. The only other major concern for the voltage hold off of the grids is with respect to damage of the surfaces due to arcing. Presently, experiments are underway at JPL to quantify the screen power supply stored energy and the maximum amount of energy that can be delivered to the surface in an arc breakdown event without significantly damaging the surface or degrading the voltage hold off capability. When complete, these experiments will provide a NEXIS PPU specification that will eliminate the possibility of damaging the grid surfaces during breakdown events. This will provide a high reliability design for the PPU-grid combination to withstand arcing and breakdown events.

Long Cathode Lifetime

The very high propellant throughput required for NEP applications demands a revolutionary approach to cathode life. In the NEXIS program a reservoir hollow cathode with an advanced emitter material will be developed to address the cathode insert failure modes. A carbon keeper electrode and operating modes designed to reduce energetic ion production are used to mitigate keeper erosion.

Hollow Cathode Operation

The electron emitter of a conventional SOA hollow cathode is an impregnated porous tungsten tube (the insert). The key to long insert life is to maintain a low temperature through the establishment of a layer of adsorbed oxygen and barium atoms that lowers the surface work function. In SOA impregnated cathodes Ba and BaO are supplied by barium calcium aluminate source material (the impregnant) incorporated in the pores of the tungsten. Gaseous Ba and BaO are released in interfacial reactions between the tungsten matrix and the impregnant, producing a temperature-dependent vapor pressure of these species inside the pores. The Ba and BaO then diffuse through the pores to the surface and replenish barium adsorbates lost by evaporation. The Ba and BaO transport rate through

the pores depends on the vapor pressure of these species at the reaction front in the porous structure. Conventional hollow cathodes depend on the control of the vapor pressure of the material in the pores. If conventional hollow cathodes are operated at too low a temperature (with inadequate self-heating at low current levels for instance) the discharge may be extinguished because there is inadequate supply of Ba and BaO. Conventional cathodes are generally designed to operate with sufficient self-heating to guarantee that there is an adequate supply of Ba and BaO. This self-heating is used to control the vapor pressure of the material in the pores. For a restricted range of operating conditions the Ba supply process is self-regulating. At too low a temperature, the supply rate is insufficient and discharge extinction occurs. Too high a temperature results in oversupply, which is not deleterious to operation but leads to more rapid exhaustion of the Ba supply.

Hollow Cathode State-of-the-Art.

SOA impregnated cathodes have demonstrated over 16,000 hours of operation on DS1 [33] and over 30,000 hours in a ground test of the DS1 flight spare engine [34]. A ground test of a similar cathode operated at higher temperatures failed after 28,000 hours [35]. The demonstrated lifetime of SOA hollow cathode insert technology is far short of that required for NEP missions.

Technical Challenges

Cathode life is limited by insert degradation and erosion of the orifice and keeper electrode [33]. There are four main processes that degrade the barium adsorbate layer and can lead to insert failure [36]:

1. *Depletion of the barium source material.* The pores of conventional cathodes contain a limited amount of material which is eventually exhausted by vapor loss through the pores to the surface or tied up in barium tungstates and the stable monobarium aluminate that do not contribute to production of Ba vapor at typical operating temperatures.
2. *Insufficient production of Ba and BaO because of*

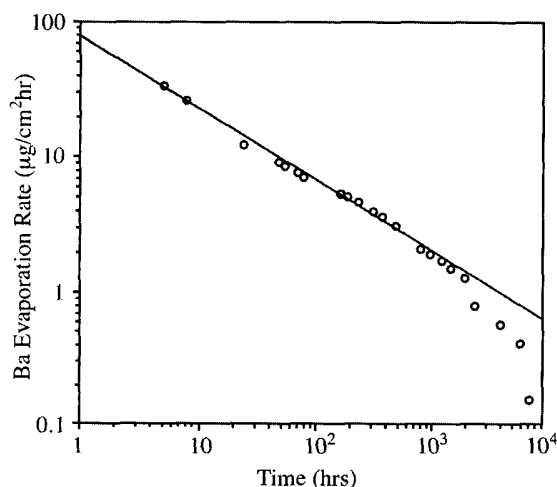


Figure 10: In conventional dispenser cathodes the barium supply rate drops as the solid-vapor front recedes into the pores.

reaction product buildup at the interface between the impregnant and the tungsten matrix. The reduction reaction that releases Ba proceeds by diffusion of reactants through this product layer. As it builds up over time, however, the diffusion rate drops. Unreacted source material may then become isolated by these product layers from the tungsten surfaces on which the reaction depends.

3. *Inadequate transport of Ba and BaO from impregnant deep in the matrix through the pores to the surface.* Conventional cathodes initially produce copious quantities of Ba and BaO. As the impregnant is consumed, however, the solid-vapor interface recedes into the pores. The vapor pressure for the given operating temperature is maintained at this interface, but the Ba and BaO must be transported through ever-increasing distances through the pores to the surface. The continually increasing conductance losses lead to reduced material flow through the pores or along the pore walls. This is shown clearly in Fig. (10), which gives the vapor production rate as a function of time for a dispenser cathode [37]. The supply rate drops as $1/(\text{time})^{1/2}$, which is consistent with diffusion limitations through the porous structure [37, 38]. Near the

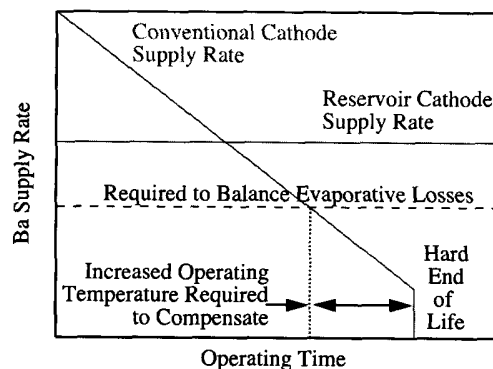


Figure 11: In conventional cathodes, failure occurs when the supply rate falls below that required to replenish evaporative losses from the surface or when the source material is exhausted. Reservoir cathodes are designed to give a constant supply rate exceeding that required and sized to prevent exhaustion of the source material during the mission.

end of the test, the supply rate drops precipitously due to complete exhaustion of the material. The implications of this behavior for cathode life are shown schematically in Fig. (11). When the supply rate drops below that required to balance losses from the surface, either the temperature must increase to compensate or the cathode fails. Increased operating temperature just accelerates the rate at which the supply is consumed. Hard failure occurs when the supply is completely exhausted.

4. *Closure of the surface pores by deposition of tungsten.* Tungsten crystals are often found on the downstream end of the insert emitter surface after long periods of operation [33, 36]. No insert failures have yet been attributed to this mass transport phenomenon, but these deposits could potentially close the pores that supply Ba and BaO in the emission zone. The tungsten is likely transported as tungsten oxide vapor, which then dissociates in the plasma near the orifice or on the hottest surfaces at the downstream end of the emitter.

Demonstrating the required cathode life is as challenging as achieving it. The remaining life capability

of standard impregnated inserts cannot be diagnosed by any established analytical procedure. In x-ray diffraction, the primary tool for phase identification, the signal from minute quantities of reaction product formed at the interface between the impregnant and tungsten along the pore walls is overwhelmed by the tungsten signal, making quantitative measurements of product concentrations virtually impossible. The life capability of conventional inserts can only be assessed by operating them to failure, introducing unacceptable technical and schedule risk for NEP applications.

Solutions

Seven innovations are used to eliminate the causes of insert failure and obtain the required cathode life.

1. *Advanced hollow cathode emitter design.* There has been no systematic development of insert technology in the history of ion propulsion. The SOA insert is a straightforward adaptation of vacuum device technology from the 1950s. While significant expenditures have been made in improving heater reliability [39] and developing insert handling and activation procedures [40, 41], no investment has been made in advancing insert technology. However, based on experience with vacuum impregnated and reservoir cathodes, hollow cathode technology does not appear to be inherently limited to the 30,000 hour lifetime achieved to date. The Tri-Service (DoD)/NASA Cathode Life Test Facility has had various types of cathodes under test for 10 to 15 years and tracks the decay in space charge-limited (SCL) current as the key indicator of cathode degradation [42]. The processes causing SCL current degradation (reduced barium adsorbate supply and surface coverage) are the same that cause hollow cathode failure. Thus, these results suggest that much more robust materials technologies are available that can significantly improve hollow cathode life. Four variables will be investigated to advance insert technology: matrix material, source material, geometry, and thermal design.

2. *Reservoir hollow cathodes.* Figure (12) shows a conceptual design that exploits all four design

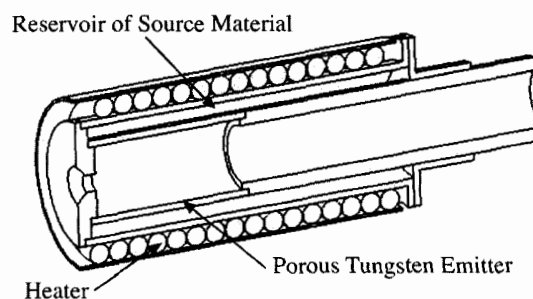


Figure 12: Reservoir hollow cathode schematic.

variables to achieve long life. The cylindrical porous emitter is a tungsten-iridium alloy, but is not impregnated with the source material. The source is contained in a reservoir surrounding the central emitter. The porous emitter serves as the emission substrate and to provide controlled passage of Ba and BaO liberated from the enclosed source material to the emitting surface. Because the source material is separated from the emitter, the porous structure provides a fixed flow resistance over the life of the cathode. The Ba and BaO supply rates are therefore much more stable than in impregnated cathodes, as observed in long duration tests of reservoir cathodes for vacuum devices [42]. A fine tungsten powder mixed with the source material serves as a reducing agent to liberate Ba and BaO, so the porous emitter structure does not need to react with the source material as it does in the impregnated cathode.

The external heater, which is the same type developed under the Space Station Plasma Contactor program and used on NSTAR [39], serves to condition the cathode after exposure to air and to preheat it prior to ignition. Thermal analysis of the conceptual design shows that it will require 110–140 W of heater power to achieve the temperatures necessary for conditioning and ignition. Because the cathode diameter is larger than that used in NSTAR or the ISS plasma contactor, the active length of the heater is longer. Even at 140 W, the power per unit length of this heater is 20% lower than in the NSTAR or ISS plasma contactor heaters. In addition, NEP missions will require over an order of magnitude fewer cycles

than the ISS contactor. The heater design is therefore very conservative and based on NSTAR/ISS heritage.

The cathode orifice diameter and emitter are sized for the cathode to be self-heating at the required operating temperature [43], just as in conventional dispenser cathodes. In principle, the reservoir could be thermally isolated from the emitter and actively controlled at a temperature that would provide the optimum Ba and BaO supply rates. However, this would introduce additional system complexities and require continuous operation of a heater. Instead, the proposed design results in very close thermal coupling of the emitter and source material, as demonstrated in Fig. (13). These thermal analysis results show that the radiation shielding results in less than a 10 degree C difference between the emitter and source temperatures over a broad range of input power levels.

The source material for the optimized reservoir cathode is chosen to oversupply the emitter surface over the entire range of expected operating temperatures, as shown schematically in Fig. (11). The reservoir is sized to support this supply rate for much longer than required to eliminate supply exhaustion as a credible failure mode. Ten candidate source material combinations identified so far span a 12 order of magnitude range in barium vapor pressures, giving plenty of options for satisfying the criterion of oversupplying the surface.

Decoupling the source material from the emitter surface in the reservoir insert eliminates all four insert failure modes. W-Ir cathodes have a lower work function than impregnated tungsten [44], which reduces the temperature. Impregnated inserts actually oversupply barium for most of their lifetime because the emitter temperature required to deliver the emission current is higher than necessary for the reactions that produce adsorbates. The excess barium does not improve performance, but does more rapidly deplete the finite supply. In a reservoir cathode, the barium supply can be very large. The conceptual reservoir cathode design contains ten times the barium of a conventional insert.

Reaction product buildup on the pore walls, which increasingly inhibits production of barium over life, is avoided in the reservoir cathode. The

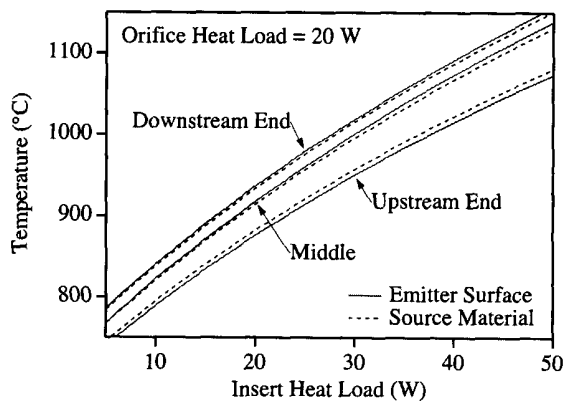


Figure 13: Thermal analysis of the proposed reservoir cathode design shows that the source and emitter temperature are strongly coupled over a broad range of emitter power input levels.

finely divided tungsten powder provides much more surface area than the interior surface area of the porous insert. Limitations in the transport of Ba and BaO are also avoided. The loosely packed, highly porous source powder offers much less resistance to vapor flow. The porous W-Ir emitter is much less reactive than pure tungsten, so the pores in the emitter do not become clogged with reaction products. This fixed flow resistance allows the supply rate to be constant as shown in Fig. (11). The supply rate of conventional dispenser cathodes drops continuously over life because the barium must flow from deeper and deeper in the porous insert. Deposition of tungsten by dissociation of tungsten oxides is also greatly reduced. W-Ir has enhanced oxidation resistance compared to pure tungsten and the lower operating temperature further reduces the oxidation rate.

Finally, reservoir cathodes enable accelerated testing. The kinetics of source material decomposition can be measured at the nominal temperature and then accelerated by operating at higher temperatures to determine the ultimate life of the supply. This is not possible with conventional impregnated cathodes because the temperature governing the reactions cannot be decoupled from that of the emitter. Raising the temperature fundamentally alters the hol-

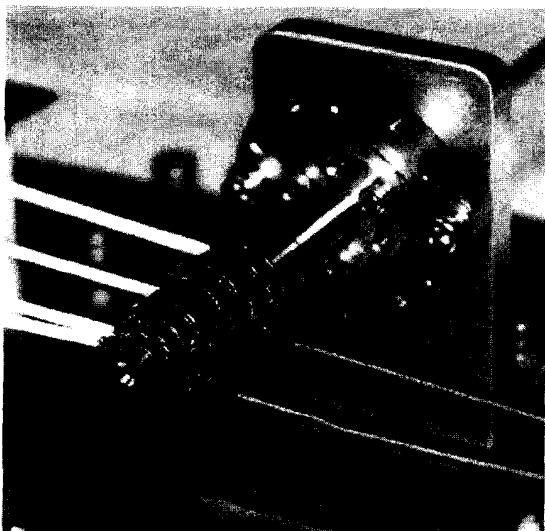


Figure 14: First proof-of-concept reservoir hollow cathode.

low cathodes operation. In addition, the method cannot be validated in a conventional hollow cathode because it is impossible to measure the extent of reaction in a porous tungsten matrix, as discussed above. The much lower tungsten content of the source material in the reservoir cathode enables quantitative measurement of reaction product concentrations to determine remaining life.

Three proof-of-concept reservoir hollow cathodes have been fabricated to demonstrate the feasibility of this approach. These cathodes are similar in size and design to that which will be used in the NEXIS engine, as shown in Fig. (14). The first of these cathodes was tested recently and demonstrated the conditioning sequence, reliable ignition and stable operation over a total emission current range of 12–37 A. Minimum xenon flow rates for stable operation ranged from 1.5 to 5.5 sccm for this current range. At all points the orifice temperature was under 1250 degrees C and the temperature at the midpoint of the outer reservoir tube was under 1060 degrees C. Figure (15) shows the cathode operating at 32 A, the highest current expected for the nominal NEXIS operating point.

3. *Advanced impregnated inserts.* An alternate ap-

proach using established hollow cathode fabrication methods will also be pursued. Impregnated inserts will be fabricated from a tungsten-iridium composition to reduce the work function. This approach lowers temperatures, reduces reactivity (slowing loss of barium and the rate of product buildup) and improves oxidation resistance, but does not physically decouple the emitter and source.

4. *Erosion-resistant carbon keepers.* Sputter-resistant graphite will be used for the cathode keepers. Graphite keepers have been used in over 3200 hours of testing in 15-cm thrusters at JPL and exhibit very little erosion [19].

5. *Discharge cathode keeper bias control.* In the NSTAR thruster, the discharge cathode keeper potential is about 20 V lower than the plasma [25]. The NEXIS keeper potential will be controlled to a value 5-10 V closer to the plasma to reduce bombarding ion energies. Recent erosion measurements in an NSTAR-like thruster using radioactive tracer techniques have shown that this approach is effective in reducing keeper erosion [45].

6. *Tailoring flows and currents to control orifice and keeper erosion.* Recent tests on board DS1 and experiments at the Aerospace Corporation and CSU [46, 47, 48, 49] reveal that the energetic ion production rate can be varied by adjusting flow rate and keeper current. These parameters will be adjusted in the NEXIS thruster to minimize erosion.

7. *Novel life validation approach.* The lifetime will be assessed by modeling and experiments. Models of the dominant wear-out processes will be developed, experimentally validated, and used to predict the life [50, 51]. The elimination of critical cathode failure modes will be verified by using in situ diagnostics to measure erosion products and with accelerated life tests of reservoir source materials. The surface layer activation erosion monitoring technique described in [45] will be used to assess cathode orifice and keeper erosion. The accelerated tests will be conducted on test articles (containers filled with source material and capped with porous W-Ir) which simulate the reservoir environment and will be carefully designed on the basis of thermochemical data. The key to the accelerated test methodology is to show that the relevant reaction rates are increased

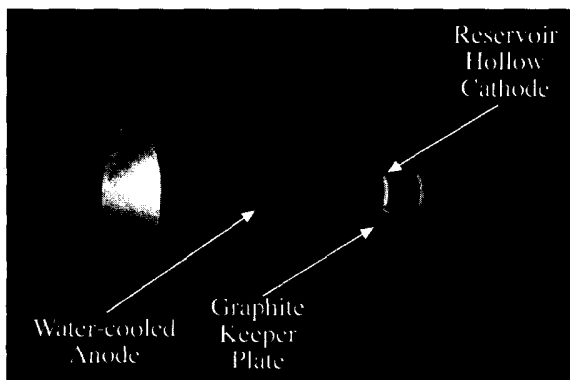


Figure 15: Proof-of-concept reservoir hollow cathode operating at 32 A, the highest current expected for the nominal NEXIS operating point.

at higher temperatures and that no new reactions are activated. The accelerated test methodology will be validated by comparison with the results of reservoir cathode wear tests of 2000 and 6000 hours duration under nominal conditions. The source material from accelerated tests simulating 2000 and 6000 hours of operation will be compared to that from the actual tests to verify that the extent of the reaction and the reaction products are the same in both cases.

High Efficiency Operation

Most of the efficiency gain is achieved by operating at much higher beam voltage, which makes the discharge loss (power required to create the ions) nearly irrelevant to the overall performance. Increases in discharge loss can be traded for improvements in propellant utilization efficiency, increasing total efficiency as shown in Fig. (16). Propellant efficiency is maximized by scaling up the discharge chamber with the same length-to-diameter as NSTAR, operating a shared neutralizer for multiple thrusters and minimizing the accelerator open area fraction.

Technical Challenges

The key to obtaining very high thruster efficiency is to maximize propellant efficiency without sacrificing thruster life.

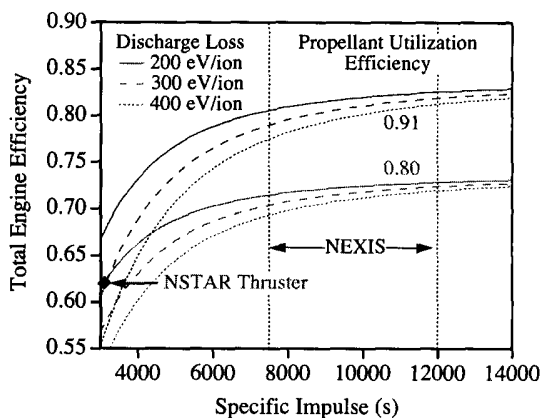


Figure 16: High thruster efficiency is achieved by operating at high propellant efficiencies at the expense of discharge loss.

Solutions

The NEXIS thruster uses three fundamental approaches:

1. *Exploit the natural improvement in discharge chamber operation by scaling.* The NEXIS thruster requires a large area plasma generator capable of high propellant utilization efficiency and low discharge loss. This is achieved by taking advantage of the natural increase in efficiency as one scales toward larger thrusters because the plasma production rate scales with the volume and the plasma loss rate scales with the surface area [52, 53]. Larger thrusters can be made more efficient, provided that the magnetic cusp confinement is designed properly and the thruster length to diameter ratio (l/d) is adequate.

To further improve the thruster performance over the SOA NSTAR baseline, the discharge anode is designed to be significantly larger in diameter than the active grid diameter. The region at the periphery of the grid near the anode surface is masked so that this very low plasma density region in the fringing magnetic-cusp fields does not limit the ion optics design or allow propellant to leak through the grid. The NEXIS thruster is designed with a 57 cm diameter grid area, and a 65 cm diameter anode chamber.

The l/d ratio is the same as in NSTAR, but the plasma profile will be greatly improved by the use of a six-ring cusp design.

An analysis of the primary electron confinement for the NEXIS 65 cm diameter anode and four or six ring cusps was conducted. As long as the cusp field exceeds a certain critical value, the primary electrons all make ionization collisions prior to being lost to the anode in the six-ring design. In addition, the six-ring design permits closing of the 50 gauss magnetic contour, which provides excellent ion confinement from radial loss to the anode surface. This further contributes to the low discharge loss of the NEXIS plasma generator design. The discharge loss for the NEXIS chamber has been analyzed using the model modified from [52]. This model requires some knowledge of the plasma parameters in the discharge, but benchmarking the code against the NSTAR results provides reasonable assumptions for the plasma temperature and profile. The NSTAR benchmark provides excellent agreement with the experimental results from the Extended Life Test. The model predicts a discharge loss of about 173 eV/ion for the NEXIS design. Plasma discharge stability analysis indicates that the four ring cusp design will be marginal if the discharge loss exceeds 200 eV/ion and discharge currents in excess of about 31 A are required. However, the six ring design provides sufficient anode area to stabilize the discharge, even if the discharge loss is 230 eV/ion and the discharge current exceed 35 A. Since the primary confinement with six cusps is acceptable and the stability is excellent, we have chosen this design. In addition, the even number of cusps in the NEXIS thruster will reduce the on-axis magnetic field compared to the 3-ring NSTAR design, which will greatly improve the plasma profile.

Increasing the propellant efficiency must be accomplished without a corresponding increase in doubly charged ions, which drives internal erosion. Scaling calculations using the model in [52] indicate that the chamber diameter, flow rates and grid area of the NEXIS thruster allow it to operate at a discharge propellant efficiency of 0.93 with no increase in double ions relative to NSTAR.

2. *Use a central shared neutralizer.* The neutralizer

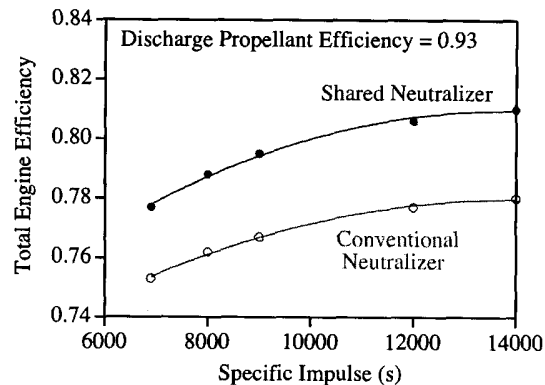


Figure 17: The shared neutralizer approach significantly increases overall efficiency.

flow reduces overall efficiency, but sufficient flow is required to create a low impedance between the neutralizer and the ion beam and to prevent neutralizer erosion. A single neutralizer providing electrons to neutralize multiple thrusters satisfies these conflicting requirements. Because the flow required for a given emission current increases slower than the current, a single neutralizer results in lower losses than individual neutralizers, improving efficiency by 3 percentage points as shown in Fig. (17). This payoff is significant enough that this option should be pursued, but it has low development risk because individual neutralizers can be used as a contingency. Neutralizer operation and location affect coupling voltage, but the thruster operation is largely independent of the neutralizer if it is properly neutralizing the beam. The discharge chamber, grid and cathode technologies can therefore be developed regardless of neutralizer approach. The single operating point for the NEP system reduces the complexity of a shared neutralizer.

3. *Match accelerator grid aperture to beamlet diameter as a function of radius.* An example of beamlet diameter variation with radius scaled from the NSTAR thruster is given in Fig. (18). The beamlets decrease in diameter with increasing radius until over-focusing starts to increase the diameters due to crossover ion trajectories. By tailoring the aperture

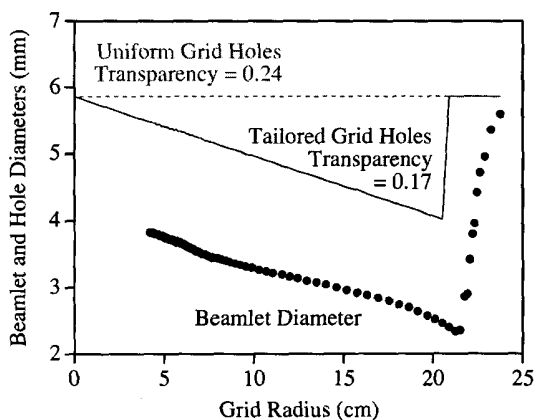


Figure 18: Tailoring the accelerator grid hole diameter with the beamlet diameter significantly decreases the open area fraction resulting in improved propellant efficiency.

diameters to follow the beamlet diameters, as suggested in Fig. (18), the open area fraction can be reduced and loss of un-ionized propellant minimized. Because the perveance margin increases radially due to the decrease in plasma density, it is possible to operate at high perveance margin on the centerline (minimizing CEX ion erosion where it is greatest) and sacrifice some margin at larger radii by decreasing aperture diameter to better contain the neutral propellant. For the example in Fig. (18), the open area fraction is decreased by 30%, increasing discharge propellant efficiency from 0.90 to 0.96 at constant discharge loss. Our design conservatively assumes that discharge propellant efficiency can be increased to 0.93.

Conclusions

Future planetary missions will demand propulsion systems with higher power processing capability, higher efficiency and longer lifetime. Although ion engines are ideally suited for this application, these requirements are a significant leap beyond what has been demonstrated for solar electric propulsion applications. The NEXIS program is designed to develop technologies which address the needs of future NEP missions. Operation at 20 kWe with spe-

cific impulses of 7500 s and greater and efficiencies exceeding 78% will be demonstrated in laboratory model and development model hardware. Extremely long engine lifetimes are enabled by the application of technologies which minimize or eliminate the wearout failure modes suffered by state-of-the-art ion thrusters. The capability to process the xenon propellant throughput required for NEP applications will be demonstrated through a combination of modeling and testing. At the end of the NEXIS second phase, these technologies should be mature enough to support an advanced development effort for flight applications.

Acknowledgements

The authors would like to acknowledge the contributions of other NEXIS team members in the planning of the program, including Professor Alec Gallimore and Dr. Tim Smith at the University of Michigan, Professor Joe Wang at Virginia Polytechnic Institute, Professor Manuel Martinez-Sanchez at MIT, Dr. Mark Crofton at the Aerospace Corporation, and Jason Vaughan and Todd Schneider at the Marshall Flight Center. The authors also thank Jim Tarter at Semicon, Inc. for his assistance in designing and fabricating the proof-of-concept reservoir cathodes. The research described in this paper was conducted in part at the Jet Propulsion Laboratory, California Institute of Technology, under contract to the National Aeronautics and Space Administration.

References

- [1] M. A. Noca and R.C. Moeller. Reaching the Outer Planets with Nuclear Electric Propulsion: Trades, Sensitivities and the Case for a Neptune System Explorer. In *Space Technology and Applications International Forum*, Albuquerque, NM, 2003. AIP Conference Proceedings 654.
- [2] L. Johnson and S. Leifer. Interstellar Exploration: Propulsion Options for Precursors and Beyond. In *50th International Astronautical Congress*, Amsterdam, The Netherlands, 1999. IAF-99-IAA.4.1.05.

- [3] K. Toki et al. Technological Readiness of Microwave Ion Engine System for MUSES-C Mission. In *27th International Electric Propulsion Conference*, Pasadena, CA, 2001. IEPC-01-174.
- [4] N. Onodera, H. Takegahara, K. Nishiyama, I. Funaki, and H. Kuninaka. Electron Emission Mechanism of Microwave Discharge Neutralizer. In *26th International Electric Propulsion Conference*, Kitakyushu, Japan, 1999. IEPC-99-160.
- [5] D. Siegfried, Feb. 2002. Personal communication.
- [6] S. Tverdokhlebov, A. Semenkin, and J.E. Polk. Bismuth Propellant Option for Very High Power TAL Thruster. In *40th Aerospace Sciences Meeting*, Reno, NV, 2002. AIAA-2002-0348.
- [7] J. S. Snyder, J.R. Brophy, D. Goebel, J. Beatty, and M. De Pano. Development and Testing of Carbon-Based Ion Optics for 30-cm Ion Thrusters. In *39th Joint Propulsion Conference*, Huntsville, AL, 2003. AIAA-2003-4716.
- [8] J. S. Snyder. Review of Carbon-Based Grid Development Activities for Ion Thrusters. In *39th Joint Propulsion Conference*, Huntsville, AL, 2003. AIAA-2003-4715.
- [9] J.R. Brophy. NASA's Deep Space 1 Ion Engine. *Rev. Sci. Inst.*, 73(2), 2002.
- [10] J.J. Wang, J.E. Polk, J.R. Brophy, and I. Katz. Three-Dimensional Particle Simulations of NSTAR Ion Optics. In *27th International Electric Propulsion Conference*, Pasadena, CA, 2001. IEPC-01-85.
- [11] P.J. Wilbur, J. Miller, C. Farnell, and V.K. Rawlin. A Study of High Specific Impulse Ion Thruster Optics. In *27th International Electric Propulsion Conference*, Pasadena, CA, 2001. IEPC-01-098.
- [12] J.A. Christensen, G. Benson, T.A. Bond, and M. Matranga. The NSTAR Ion Propulsion Subsystem for DS1. In *35th Joint Propulsion Conference*, Los Angeles, CA, 1999. AIAA-99-2972.
- [13] J.R. Brophy, J.E. Polk, and V.K. Rawlin. Ion Engine Service Life Validation by Analysis and Testing. In *32nd Joint Propulsion Conference*, Lake Buena Vista, FL, 1996. AIAA-96-2715.
- [14] R. Deltschew, M. Tartz, V. Plicht, E. Hartmann, H. Neumann, H. Leiter, and J. Esch. Sputter Characteristics of Carbon-Carbon Compound Material. In *27th International Electric Propulsion Conference*, Pasadena, CA, 2001. IEPC-01-118.
- [15] J. Meserole and D. Hedges. Comparison of Erosion Rates of Carbon-Carbon and Molybdenum Ion Optics. In *23rd International Electric Propulsion Conference*, Seattle, WA, 1993. AIAA-93-111.
- [16] C.E. Garner, J.R. Brophy, and L.C. Pless. Fabrication and Testing of Carbon-Carbon Grids for Ion Engines. In *28th Joint Propulsion Conference*, Nashville, TN, 1992. AIAA-92-3149.
- [17] J. Mueller, D.K. Brown, C.E. Garner, and J.R. Brophy. Fabrication of Carbon-Carbon Grids for Ion Optics. In *23rd International Electric Propulsion Conference*, Seattle, WA, 1993. AIAA-93-112.
- [18] J. Mueller, J.R. Brophy, and D.K. Brown. Performance Characterization of 15-cm Carbon-Carbon Composite Grids. In *30th Joint Propulsion Conference*, Indianapolis, 1994. AIAA-94-3118.
- [19] J. Mueller, J.R. Brophy, and D.K. Brown. Endurance Testing and Fabrication of Advanced 15-cm and 30-cm Carbon-Carbon Composite Grids. In *31st Joint Propulsion Conference*, San Diego, CA, 1995. AIAA-95-2660.
- [20] J.R. Brophy, J. Mueller, and D.K. Brown. Carbon-Carbon Ion Engine Grids with Non-Circular Apertures. In *31st Joint Propulsion*

- Conference*, San Diego, CA, 1995. AIAA-95-2262.
- [21] J. Mueller, J.R. Brophy, and D.K. Brown. Design, Fabrication and Testing of 30-cm Dished Carbon-Carbon Ion Engine Grids. In *32nd Joint Propulsion Conference*, Lake Buena Vista, FL, 1996. AIAA-96-3204.
- [22] I. Funaki et al. 20mN-class Microwave Discharge Ion Thruster. In *27th International Electric Propulsion Conference*, Pasadena, CA, 2001. IEPC-01-103.
- [23] I. Funaki et al. Verification Tests of 10-cm-Diam. Carbon-Carbon Composite Grids for Microwave Discharge Ion Thruster. In *26th International Electric Propulsion Conference*, Kitakyushu, Japan, 1999. IEPC-99-164.
- [24] M.J. Patterson, R.F. Roman, and J.E. Foster. Ion Engine Development for Interstellar Precursor Missions. In *36th Joint Propulsion Conference*, Huntsville, AL, 2000. AIAA-2000-3811.
- [25] J.E. Polk, J.R. Anderson, J.R. Brophy, V.K. Rawlin, M.J. Patterson, and J.S. Sovey. The Results of an 8200 Hour Wear Test of the NSTAR Ion Thruster. In *35th Joint Propulsion Conference*, Los Angeles, CA, 1999. AIAA-99-2446.
- [26] J.R. Brophy, I. Katz, J.E. Polk, and J.R. Anderson. Numerical Simulations of Ion Thruster Accelerator Grid Erosion. In *38th Joint Propulsion Conference*, Indianapolis, IN, 2002. AIAA-99-4261.
- [27] V.K. Rawlin. NSTAR Memorandum: Screen Grid Wear at Low Flow and High Beam Current Conditions. Technical report, Lewis Research Center, Cleveland, OH, 1996.
- [28] J.R. Brophy, C.E. Garner, J.E. Polk, and J. Weiss. The Ion Propulsion System on NASA's Space Technology 4/Challengier Comet Rendezvous Mission. In *35th Joint Propulsion Conference*, Los Angeles, CA, 1999. AIAA-99-2856.
- [29] J.E. Polk, N.R. Moore, L.E. Newline, J.R. Brophy, and D.H. Ebbeler. Probabilistic Analysis of Ion Engine Accelerator Grid Life. In *23rd International Electric Propulsion Conference*, Seattle, WA, 1993. AIAA-93-176.
- [30] J.E. Polk, N.R. Moore, J.R. Brophy, and D.H. Ebbeler. The Role of Analysis and Testing in the Service Life Assessment of Ion Engines. In *24th International Electric Propulsion Conference*, Moscow, Russia, 1995. IEPC 95-228.
- [31] J.R. Anderson, J.E. Polk, and J.R. Brophy. Service Life Assessment for Ion Engines. In *25th International Electric Propulsion Conference*, Cleveland, OH, 1997. IEPC 97-049.
- [32] N.R. Moore, D.H. Ebbeler, L.E. Newlin, S. Sutharshana, and M. Creager. An Improved Approach for Flight Readiness Assessment—Methodology for Failure Risk Assessment and Application Examples. Technical Report 92-15, Jet Propulsion Laboratory, California Institute of Technology, Pasadena, CA, 1992.
- [33] J.E. Polk, D. Brinza, R.Y. Kakuda, J.R. Brophy, I. Katz, J.R. Anderson, V.K. Rawlin, M.J. Patterson, J. Sovey, and J. Hamley. Demonstration of the NSTAR Ion Propulsion System on the Deep Space One Mission. In *27th International Electric Propulsion Conference*, Pasadena, CA, 2001. IEPC-01-075.
- [34] A. Sengupta, J.R. Brophy, and K.D. Goodfellow. Status of the Extended Life Test of the Deep Space 1 Flight Spare Ion Engine after 25,700 Hours of Operation. In *39th Joint Propulsion Conference*, Huntsville, AL, 2003. AIAA-2003-4558.
- [35] T.R. Sarver-Verhey. 28,000 Hour Xenon Hollow Cathode Life Test Results. In *25th International Electric Propulsion Conference*, Cleveland, OH, 1997. IEPC 97-168.
- [36] T.R. Sarver-Verhey. Destructive Evaluation of a Xenon Hollow Cathode After a 28,000 Hour Life Test. In *34rd Joint Propulsion Conference*, Cleveland, OH, 1998. AIAA-98-3482.

- [37] E.S. Rittner, W.C. Rutledge, and R.H. Ahlert. On the Mechanism of Operation of the Barium Aluminate Dispenser Cathode. *J. Appl. Phys.*, 28(12):1468–1473, 1957.
- [38] P. Palluel and A.M. Schroff. Experimental Study of Impregnated Cathode Behavior, Emission and Life. *J. Appl. Phys.*, 51(5):2894–2902, 1980.
- [39] S.D. Kovaleski, M.J. Patterson, G.C. Soulas, and T.R. Sarver-Verhey. A Review of Testing of Hollow Cathodes for the International Space Station Plasma Contactor. In *27th International Electric Propulsion Conference*, Pasadena, CA, 2001. IEPC-01-271.
- [40] W.L. Ohlinger and K.M. Rebstock. Barium Calcium Aluminate Impregnant Materials: Interactions with Sea-Level Ambient Atmosphere and Decomposition Behaviors of Reaction Products. In *30th Joint Propulsion Conference*, Indianapolis, 1994. AIAA-94-3135.
- [41] W.L. Ohlinger and K.M. Rebstock. Barium Calcium Aluminate Impregnant Materials: Thermal Analysis of Hydrolysis Products. In *1994 Tri-Service/NASA Cathode Workshop*, Cleveland, OH, 1994.
- [42] L. Dressman. Tri-Service/NASA Cathode Life Test Facility Annual Report, January 2000-January 2001. Technical Report Code 80943, Naval Surface Warfare Center, Crane Division, Crane, IN, 2001.
- [43] V.K. Rawlin et al. High Current Hollow Cathodes for Ion Thrusters. In *19th International Electric Propulsion Conference*, Colorado Springs, CO, USA, 1987. AIAA-87-1072.
- [44] B.K. Vancil, W.L. Ohlinger, R.A. Mueller, R.A. Steele, and E.G. Wintucky. The Metallurgical Properties of Tungsten-Iridium Cathodes. In *International Vacuum Electron Sources Conference-1998*, Tsukuba, Japan, 1998.
- [45] R.D. Kolasinski and J.E. Polk. Characterization of Cathode Keeper Wear by Surface Layer Activation. In *39th Joint Propulsion Conference*, Huntsville, AL, 2003. AIAA-2003-5144.
- [46] J.R. Brophy, D.E. Brinza, J.E. Polk, M.D. Henry, and A. Sengupta. The DS1 Hyper-Extended Mission. In *38th Joint Propulsion Conference*, Indianapolis, IN, 2002. AIAA-99-3673.
- [47] M.W. Crofton. Preliminary Mass Spectrometry of a Xenon Hollow Cathode. *J. Propulsion and Power*, 16(1):157–159, 2000.
- [48] I. Kameyama. Effects of External Flow near High-Current Hollow Cathodes on Ion Energy Distributions. In *25th International Electric Propulsion Conference*, Cleveland, OH, 1997. IEPC 97-173.
- [49] I. Kameyama. Effects of Neutral Density on Energetic Ions Produced Near High-Current Hollow Cathodes. Technical Report NASA CR-204154, Colorado State University, Fort Collins, CO 80523, 1997.
- [50] I. Katz, J. Anderson, D.M. Goebel, R. Wirz, and A. Sengupta. Plasma Generation Near an Ion Engine Discharge Chamber Hollow Cathode. In *39th Joint Propulsion Conference*, Huntsville, AL, 2003. AIAA-2003-5161.
- [51] I. Katz, J.R. Anderson, J.E. Polk, and J.R. Brophy. A Model of Hollow Cathode Plasma Chemistry. In *38th Joint Propulsion Conference*, Indianapolis, IN, 2002. AIAA-99-4241.
- [52] J.R. Brophy. Ion Thruster Performance Model. Technical Report NASA CR-174810, Colorado State University, Fort Collins, CO 80523, 1984.
- [53] H.R. Kaufman. Technology of Electron Bombardment Ion Thrusters. *Advances in Electronics and Electron Physics*, 36:p. 364, 1974.